J. Fluid Mech. (1990), vol. 217, pp. 213–239
Printed in Great Britain

Buoyancy-driven fluid fracture: similarity solutions for the horizontal and vertical propagation of fluid-filled cracks

By JOHN R. LISTER†
Research School of Earth Sciences, Australian National University, PO Box 4, Canberra 2601, ACT, Australia

(Received 11 July 1989 and in revised form 8 January 1990)

Buoyancy-driven flows resulting from the introduction of fluid of one density into a crack embedded in an elastic solid of different density are analysed. Scaling arguments are used to determine the regimes in which different combinations of the buoyancy force, elastic stress, viscous pressure drop and material toughness provide the dominant pressure balance in the flow. The nonlinear equations governing the shape and rate of spread of the propagating crack are formulated for the cases of vertical propagation of buoyant fluid released into a solid of greater density and of lateral propagation of fluid released at an interface between an upper layer of lesser density and a lower layer of greater density. Similarity solutions of these equations are derived under the assumption that the volume of fluid is given by Qt^{α}, where Q and α are constants. Both laminar and turbulent flows are considered.

Fluid fracture is an important mechanism for the transport of molten rock from the region of production in the Earth's mantle to surface eruptions or near-surface emplacement. The theoretical solutions provide simple models which describe the relation between the elastic and fluid-mechanical phenomena involved in the vertical transport of melt through the Earth's lithosphere and in the lateral intrusion of melt at a neutral-buoyancy level close to the Earth's surface.

1. Introduction

The transport of molten rock, or magma, by fissures opened by fluid-induced fracture of the Earth's lithosphere is an important and intriguing phenomenon. It is accepted that this 'magma-fracture' is responsible for the transport through the lithosphere of nearly all of the melt produced in the underlying mantle. However, the impossibility of making direct observations of the geometry of the underground conduits and of the dynamics of their formation has limited our understanding of the parameters and physical balances that control the propagation of the fissure system. These factors determine, for example, whether the melt is erupted onto the Earth's surface or whether it is emplaced at some depth in the crust. It is our purpose in this paper to analyse the governing balance of stresses for a propagating, fluid-filled fracture and to present solutions of two problems of crack propagation which are directly relevant to the transport of magma through fissures.

We consider melts that are produced in the upper regions of the Earth's mantle, some tens or hundreds of kilometres below the surface. Such melts are less dense than

† Present address: Institute of Theoretical Geophysics *and* Department of Applied Mathematics and Theoretical Physics, University of Cambridge, Silver Street, Cambridge CB3 9EW, UK.

the surrounding rock and rise to collect at the base of the overlying cold and brittle lithosphere. Here, an accumulated reservoir of magma is observed as a region of anomalously low seismic velocities. Subsequent transport of the magma towards the surface takes place through fissures, or dykes, which are initiated in the walls of the reservoir and propagate upwards through the lithosphere, driven by the buoyancy of the magma. The rate of propagation of the dyke tip may be inferred to be of order a few metres per second from seismic signals generated by the fracture of the country rock (Aki, Fehler & Das 1977; Shaw 1980); these values are consistent with the velocities that are needed to explain the size and composition of mineral fragments carried by the flow (Carmichael *et al.* 1977; Spera 1980; Pasteris 1984). During this stage of magma transport, we are concerned with the vertical propagation of a buoyant fluid-filled crack which is fed from a source at its base.

The density of the lithosphere decreases near the Earth's surface and most melts are more dense than the uppermost layers. In such cases, the propagation of a vertical dyke is arrested near the neutral-buoyancy level of the melt (Ryan 1987; Walker 1989) and the dyke may feed into a storage chamber of magma, located a few kilometres below the Earth's surface. As the chamber inflates slowly, the internal pressure increases. Episodically, the pressure is relieved as cracks are initiated in the walls of the chamber causing new dykes to propagate away from the chamber. The stress field and surface topography near the chamber may be such that these dykes reach the surface and cause fissure eruptions. More commonly, it is observed that the dykes propagate laterally rather than vertically (Rubin & Pollard 1987) and that the majority of the magma fails to reach the surface. During this stage of magma transport, we are interested in the lateral propagation of a crack in a stratified solid, where the crack is fed from one end with fluid at its neutral-buoyancy level in the solid.

The subject of dyke propagation is clearly of considerable interest for our understanding of the evolution of the Earth's crust and mantle and of the origins of the igneous intrusions that contain many of the world's valuable ore deposits. Many previous studies have examined the exposed remains of solidified intrusions (e.g. Pollard & Muller 1976; MacDonald *et al.* 1988; Reches & Fink 1988) and related them to theoretical solutions for the shape of a stationary fluid-filled crack (Weertman 1971; Pollard & Holzhausen 1979; Rubin & Pollard 1987; Pollard 1987). These solutions are sometimes extended to give a quasi-static description of a propagating crack in which the criterion for propagation is that the stress intensity at the edge of the crack exceeds a critical value for the material. However, dynamical effects, such as the viscous pressure drop in the fluid, are ignored. Some qualitative experiments (Fiske & Jackson 1972; Maaloe 1987) have investigated the shape of a propagating crack but it seems unlikely that these were in the appropriate physical regime for dyke propagation. Solutions that do incorporate the dynamical interaction between the fluid-mechnical and elastic forces have been derived for two-dimensional cracks in which buoyancy forces are negligible (Spence & Sharp 1985) or which propagate vertically, driven by the buoyancy of their contents (Lister 1990*a*; Spence & Turcotte 1989).

In this paper we begin with a general investigation and analysis of the pressure scales associated with the propagation of cracks. A number of dynamical regimes are identified, characterized by different balances between the buoyancy force, elastic stress, viscous pressure drop and the toughness of the solid material. It is shown that, for geophysical parameters, the pressures associated with fluid flow cannot be neglected in a description of the dynamics of dyke formation. In §§3 and 4 we present analytic solutions appropriate to the geophysical regime for the cases of vertical propagation of fluid released into a uniform solid of greater density and of lateral propagation of fluid released at its neutral-buoyancy level into a stratified solid (figure 1*a*, *b*). The source of fluid is taken to be point-like in comparison to the scale of the crack and these solutions thus complement the two-dimensional solutions (Spence & Sharp 1985; Lister 1990*a*; Spence & Turcotte 1989), which are relevant to line sources. The solutions given in §§3 and 4 are derived under the assumption that the flow is laminar. In §5 we extend these calculations to allow for the possibility that the flow in the crack is turbulent.

Since our intention is to demonstrate the interactive balance between the fluid-mechanical and elastic forces in a propagating crack, we neglect in our analysis the possible complications of solidification or melting at the walls of the crack. Analysis of flow in a dyke after it has become established shows that these complications may be a significant influence in the lithosphere (Huppert & Sparks 1985; Bruce & Huppert 1989, 1990).

The theoretical solutions for the propagation of fluid-filled cracks are discussed in §6 and are shown to be analogous to solutions for the spread of viscous gravity currents (Smith 1973; Huppert 1982*a*; Lister & Kerr 1989). The geophysical implications of the analysis are assessed briefly, though a more detailed discussion of this application will be given in Lister (1990*b*).

2. Preliminary analysis of fluid-fracture and crack propagation

Before deriving analytical solutions for the propagation of a fluid-filled crack in two specific geometries, we wish to present a general discussion of crack propagation which will allow the analytical solutions to be seen in context. First, we discuss the magnitudes of the viscous stresses which play a role in fluid fracture, derive the conditions which delineate the different propagation regimes and, using typical geophysical values for the parameters, determine which regimes are most relevant to the transport of magma in the lithosphere. Secondly, we derive the equations that give the thickness and flow rate in a long, thin fluid-filled crack in terms of the pressure distribution in the fluid.

2.1. *Analysis of pressure scales and flow regimes*

Consider a fluid-filled crack embedded in an infinite elastic solid. Suppose that the solid has shear modulus G, Poisson's ratio ν, density ρ_s, and stress-intensity factor (defined below) K and that the fluid is incompressible and has dynamic viscosity μ, density ρ_f and volume $V(t)$. We assume that V may be calculated from a known rate of injection of fluid into the crack. Let $\Delta\rho = \rho_s - \rho_f$ and $m = G/(1-\nu)$. For simplicity, suppose that the crack lies in a vertical plane and define h to be the vertical extent, b the horizontal extent and w the width of the crack. It is assumed, and can easily be verified from the resultant solutions, that $w \ll b, h$. Let u be a typical velocity scale for the fluid flow and let l denote the extent of the crack (either b or h depending on the context). For the moment we shall consider only laminar flow; a discussion of turbulent flow is deferred to §5.

The following analysis is presented in general terms so as to allow wide applicability of the results. Where appropriate, however, we have used the parameter values $m = 10^{10}$ Pa, $K = 10^6$ Pa m$^{\frac{1}{2}}$, $\mu = 10^2$ Pa s and $\Delta\rho = 300$ kg m^{-3} to ascertain whether a particular expression is relevant in a geophysical setting. Injection rates

$\mathrm{d}V/\mathrm{d}t$ vary greatly from $O(1\ \mathrm{m^3\,s^{-1}})$ (Rubin & Pollard 1987) to $O(10^6\ \mathrm{m^3\,s^{-1}})$ (Swanson, Wright & Helz 1975).

The relative magnitudes of four pressure scales control the regime of crack propagation. These are (i) the pressure required to open the crack against elastic forces

$$\Delta P_{\mathrm{e}} \sim \frac{mw}{l}, \tag{2.1}$$

where l is the smaller of b and h, (ii) the hydrostatic pressure due to the density difference

$$\Delta P_{\mathrm{h}} \sim g\,\Delta\rho h, \tag{2.2}$$

(iii) the viscous pressure drop caused by flow in the crack

$$\Delta P_{\mathrm{v}} \sim \frac{\mu u l}{w^2}, \tag{2.3}$$

where l is the distance from the point of injection to the crack tip, and (iv) a crack-extension pressure defined by

$$\Delta P_{\mathrm{c}} \sim \frac{K}{l^{\frac{1}{2}}}. \tag{2.4}$$

This last pressure is that required for the square-root singularity in the stress field immediately ahead of the crack tip to have strength K, where K is a material-dependent parameter called the critical stress-intensity factor (Irwin 1958). If the strength of the singularity were any smaller than this value then the crack would not propagate. Conversely, if the strength of the singularity were maintained at a larger value then the crack would propagate at about 40 % of the speed of sound in the solid (Anderson & Grew 1977), which is inconsistent with a mechanism of fracture driven by viscous flow into the crack tip.

In the Earth's lithosphere, there may be pre-existing deviatoric stresses due to tectonic motions. These stresses often determine the initial orientation of the crack but, unless they vary significantly along the length of the crack, they have little influence on the subsequent dynamics of the propagation of the crack (Lister 1990*b*).

Conservation of volume in the fluid leads to the relations

$$u \sim \frac{l}{t}, \tag{2.5}$$

$$hbw \sim V, \quad \text{(three-dimensional flows)} \tag{2.6a}$$

$$lw \sim V, \quad \text{(two-dimensional flows)} \tag{2.6b}$$

where t is the time since the initiation of the crack. These relations, together with the estimates (2.1)–(2.4) of the pressure scales, are sufficient to determine the dimensions and rate of spread of a fluid-filled crack in the different parameter regimes.

Suppose, first, that the hydrostatic pressure is negligible in comparison with the other pressure scales so that we may take $\Delta P_{\mathrm{h}} = 0$. The width of the crack is then given by one of two possible balances: $\Delta P_{\mathrm{e}} \sim \Delta P_{\mathrm{c}}$ or $\Delta P_{\mathrm{e}} \sim \Delta P_{\mathrm{v}}$. If viscous forces are negligible then the fluid pressure is given by (2.1) and the crack will extend to a length given by (2.4) subject to the constraint that the volume of the crack is given by (2.6). Thus

$$l \sim \left(\frac{Vm}{K}\right)^{2/(2n+1)}, \tag{2.7}$$

where $n = 0$ for a two-dimensional crack and $n = 1$ for an axisymmetric crack. Alternatively, if the crack-extension pressures are negligible then the extent of the crack is governed by a balance between the viscous and the elastic pressures. Using (2.1), (2.3), (2.5) and (2.6), we obtain

$$l \sim \left(\frac{V^3 mt}{\mu}\right)^{1/(3n+6)}. \tag{2.8}$$

If we assume that $V \propto t^{\alpha}$ then three possibilities arise depending on the relative sizes of α and a critical value α_c: if $\alpha < \alpha_c$ then the crack is initially limited by the viscous pressure drop and propagates according to (2.8) but at later times is limited by the resistance to crack extension and propagates according to (2.7); if $\alpha > \alpha_c$ the crack initially propagates according to (2.7) and later propagates according to (2.8); if $\alpha = \alpha_c$ then the viscous and crack-extension pressures maintain the same relative magnitudes for all times. In this final case, a similarity solution including both effects is possible and has been calculated for the two-dimensional geometry by Spence & Sharp (1985). Here $\alpha_c = 1$ (two-dimensional) or $\alpha_c = \frac{5}{3}$ (axisymmetric). In general, comparison of (2.7) and (2.8) shows that viscous pressures will dominate crack-extension pressures when

$$\frac{V}{tl^n} \gg \frac{K^4}{\mu m^3}. \tag{2.9}$$

For the parameters given, the right-hand side of (2.9) is 10^{-8} m^2 s^{-1} so this condition is nearly certain to be satisfied in geophysical applications.

Secondly, we suppose that the crack is stationary or slowly moving. In this case we may neglect ΔP_v and look for a balance between the elastic pressure ΔP_e and the sum of the hydrostatic pressure ΔP_h and an excess pressure ΔP_0 in the fluid. Solutions for a two-dimensional crack ($b = \infty$) are given by Weertman (1971). From these it may be seen that if $h > 4\Delta P_0/g\,\Delta\rho$ then the lower tip of the crack will close and if $(\frac{1}{2}h)^{\frac{1}{2}} > K/(\Delta P_0 + \frac{1}{4}g\,\Delta\rho h)$ then the upper tip will crack open. (Similar scalings will apply to a crack with finite breadth $b = 0(h)$.) It follows that a stable crack has a maximum height and width given by

$$h \sim \left(\frac{K}{g\,\Delta\rho}\right)^{\frac{2}{3}}, \quad w \sim \left(\frac{K^4}{g\,\Delta\rho m^3}\right)^{\frac{1}{3}}. \tag{2.10}$$

For the geophysical parameters given above $h \sim 50$ m and $w \sim 0.7 \times 10^{-3}$ m. It is clear that such narrow cracks would be incapable of transporting significant volumes of magma through the lithosphere.

We see from (2.9) and (2.10) that ΔP_c is negligible and that ΔP_v provides the dominant resistance for the propagation of both vertical and horizontal cracks in the lithosphere. It remains to determine whether the flow is driven by the elastic or by the hydrostatic pressures. From (2.1) and (2.2) we find that $\Delta P_h \sim \Delta P_e$ when

$$\frac{h^2}{w} \sim \frac{m}{g\,\Delta\rho}, \tag{2.11}$$

the right-hand side of which is typically 3×10^6 m. If h^2/w is much less than this value then we may neglect ΔP_h and the propagation of the crack is given by (2.8). However, the vertical extent of feeder dykes through the lithosphere is such that h^2/w is likely to be greater than 3×10^6 m (e.g. $h>2$ km, $w<1$ m) in which case we may neglect ΔP_e and the dominant pressure balance is between ΔP_h and ΔP_v. The walls of the crack are held apart against the elastic pressure ΔP_e by a small overpressure given by the incompressibility of the fluid; elastic effects are only significant near the crack tip where they play a role in the resolution of the leading kinematic shock wave. Using (2.2), (2.3), (2.5) and (2.6*b*), we find that the rate of propagation of a two-dimensional crack with $b=\infty$ is given by

$$h \sim \left(\frac{g\,\Delta\rho V^2 t}{\mu}\right)^{\frac{1}{3}}. \tag{2.12}$$

The solutions for the case of constant influx of fluid and the shape of the elastic shock wave at the crack tip have been calculated by Lister (1990*a*). In general, the dominant balance between ΔP_h and ΔP_v is equivalent to that governing the flow of a fluid down an inclined plane and, consequently, the thickness of the crack is governed by the kinematic-wave equation (Huppert 1982*b*). If the flow rate Q from the source region varies with time then the thickness near the source varies according to $w\sim(Q\mu/g\,\Delta\rho)^{\frac{1}{3}}$ and these variations in thickness propagate away from the source at a velocity $g\,\Delta\rho w^2/\mu$. The solution for the particular case of a crack of constant volume has been derived by Spence & Turcotte (1989) under the assumption that the leading elastic shock may be neglected.

Having shown that the vertical flow in dykes is governed by a balance between ΔP_h and ΔP_v, we now discuss the balance that determines the lateral extent b of the crack. For simplicity, we consider only the case of a crack fed by a fixed volume flux Q. As the crack rises, it will tend to spread laterally owing to the variations in w and ΔP_e in any horizontal cross-section. (This spread is analogous to the downstream spreading of a gravity current on an inclined plane due to cross-stream variations in the thickness of the current.) Two pressure balances are possible. First, b could be determined by a balance between the crack-extension pressure (2.4) and ΔP_e. The consequent width and breadth of the crack may be found from the scaling estimates to be given by

$$w \sim \left(\frac{K^2\mu Q}{m^2 g\,\Delta\rho}\right)^{\frac{1}{5}}, \qquad b \sim \left(\frac{m^3\mu Q}{K^3 g\,\Delta\rho}\right)^{\frac{2}{5}}. \tag{2.13a, b}$$

Secondly, b could be determined by a balance between ΔP_e and ΔP_v so that the horizontal fluid velocity u_x is given by (2.1) and (2.3). The shape of the crack is defined by $u_x/u_z \sim \mathrm{d}b/\mathrm{d}z \sim b/z$, where z is the height above the source of fluid and, provided that $b \ll z$, the vertical velocity u_z is found from (2.1) and (2.2). We obtain

$$w \sim \left(\frac{Q^3\mu^3}{(g\,\Delta\rho)^2 mz}\right)^{\frac{1}{10}} \quad (z<h) \tag{2.14a}$$

$$b \sim \left(\frac{Q\mu m^3 z^3}{(g\,\Delta\rho)^4}\right)^{\frac{1}{10}} \quad (z<h) \tag{2.14b}$$

$$h \sim \left(\frac{(g\,\Delta\rho)^3 Q^3 t^5}{\mu^2 m}\right)^{\frac{1}{6}}. \tag{2.14c}$$

There is a transition at $z \sim m^3 Q\mu/K^4$ from behaviour given at shallow heights by (2.14) to behaviour given at greater heights by (2.13). For geophysical parameters the transition height is $10^8 Q$ m, where Q ranges from of order 1 $\mathrm{m^3\,s^{-1}}$ to much larger values. Therefore, the transition height is much greater than the thickness of the lithosphere and so the lateral spread is given by (2.14). An analytical solution for this regime will be presented in §3.

An important consequence of the dominant vertical balance between ΔP_{h} and ΔP_{v} is that lithospheric cracks have little tendency to propagate through a level at which the density of the solid decreases below that of the melt. If such a crack reaches the neutral-buoyancy level of the melt then the vertical overshoot of the crack beyond this level will be given by (2.11). Subsequently, the crack will propagate in a predominantly horizontal direction along the neutral-buoyancy level. Solutions for this flow are given in §4.

In conclusion, the scaling arguments show that the resistance to fracture K is unimportant in geophysical applications; thin fractures could propagate much faster than magma would be able to intrude behind them. Resistance to fracture is only likely to be relevant during the initial nucleation and growth of a crack while it is still very short. Once the crack has grown to a sufficiently large vertical extent, as defined by (2.11), the dominant balance for the vertical motion is between ΔP_{h} and ΔP_{v}; the rise is then given by (2.12) or (2.14) depending on whether the source region is linear or point-like in comparison to the scale of the crack. If the crack rises to a density interface at which the density difference between the solid and fluid is reversed then (2.11) describes the height to which the crack can penetrate the upper layer; any further spread will be horizontal and along the interface.

2.2. *Theoretical results for thin cracks*

We consider a crack of width $2w(x,z)$ lying in the plane $y=0$ and derive the equations that govern the elastic and fluid-mechanical responses to the fluid pressure p in the crack. These linked equations will be used in §§3 and 4 for the solution of two crack-propagation problems in the geophysically relevant regimes identified above.

We assume that the crack is sufficiently narrow and the fluid sufficiently viscous that

$$\rho_{\mathrm{f}}\, w^3 |\nabla w \cdot \nabla p|/\mu^2 \ll 1.$$

It follows that the flow satisfies the conditions of lubrication theory and, consequently, that p is a function only of x and z and the fluid velocity is given by

$$\boldsymbol{u} = -\frac{1}{2\mu}(w^2 - y^2)\,\nabla p. \tag{2.15}$$

The variation of the thickness of the crack with time is given by the continuity equation $2\,\partial w/\partial t + \nabla \cdot \boldsymbol{q} = 0$, where $\boldsymbol{q}(x,z)$ is the local volume flux. After substitution from (2.15), we obtain

$$\frac{\partial w}{\partial t} = \frac{1}{3\mu}\nabla \cdot (w^3 \nabla p). \tag{2.16}$$

Now suppose that the crack is two-dimensional and has width $2w(s)$, where s may be either x or z. The assumption of two-dimensionality is appropriate for a crack rising from a long, linear source (Lister 1990*a*) or as a local approximation to the shape of a crack with $h \gg b$ (see §3) or $b \gg h$ (see §4). The elastic pressure in the plane $y = 0$ is given by

$$p = -m\mathscr{H}\{\mathrm{d}w/\mathrm{d}s\} \tag{2.17}$$

(Muskhelishvili 1975), where $\mathscr{H}\{\cdot\}$ denotes the Hilbert transform. This transform may be inverted to give $\mathrm{d}w/\mathrm{d}s$ in terms of the fluid pressure p. Depending on whether the crack is infinite, semi-infinite or finite in extent we obtain

$$\frac{\mathrm{d}w}{\mathrm{d}s} = \frac{1}{m}\mathscr{H}\{p\} \qquad (w \neq 0 \quad \forall s) \tag{2.18a}$$

$$= \frac{1}{m\pi}\int_0^\infty p(\sigma)\left(\frac{\sigma}{s}\right)^{\frac{1}{2}}\frac{\mathrm{d}\sigma}{\sigma - s} + \frac{c_1}{s^{\frac{1}{2}}} \qquad (w \neq 0 \quad \text{for } s > 0) \tag{2.18b}$$

$$= \frac{1}{m\pi}\int_{-s_*}^{s_*} p(\sigma)\left(\frac{s_*^2-\sigma^2}{s_*^2-s^2}\right)^{\frac{1}{2}}\frac{\mathrm{d}\sigma}{\sigma - s} + \frac{c_2}{(s_*^2-s^2)^{\frac{1}{2}}} \qquad (w \neq 0 \quad \text{for } |s| < s_*). \tag{2.18c}$$

The constants c_1 and c_2 are found from the boundary conditions that w is finite as $s \rightarrow \infty$ and $w = 0$ at the edges of the crack.

3. Vertical propagation of a crack filled with buoyant fluid

Consider the release of an incompressible fluid of density ρ_f into a crack in an infinite elastic solid of greater density ρ_s. (We use the notation of the previous section for the other material parameters.) Suppose that the rate of release is such that the total volume of fluid is Qt^α. The fluid will rise, driven by its buoyancy, thus causing a planar crack to propagate upwards. We define the origin of coordinates to be the point of release and take the z-direction to be vertically upwards (figure 1*a*). Let the crack occupy $|y| < w(x, z, t)$ and let the edges of the crack be at $x = \pm b(z, t)$. We assume that the crack has propagated a sufficient distance that the height h of the crack satisfies $h \gg b$. As we noted in the previous section, $b \gg w$.

The fluid pressure is given by the sum of the buoyancy force and the elastic pressure exerted by the solid. Since $h \gg b$, the crack may be treated as being locally two-dimensional and the elastic pressure is given by (2.17), where the Hilbert transform is taken with respect to x. Thus the total pressure is given by

$$p = -g\,\Delta\rho z - m\mathscr{H}\left\{\frac{\partial w}{\partial x}\right\}. \tag{3.1}$$

We substitute into (2.16) and use the global conservation of fluid volume to obtain

$$3\mu\frac{\partial w}{\partial t} + g\,\Delta\rho\frac{\partial w^3}{\partial z} + m\frac{\partial}{\partial x}\left(w^3\frac{\partial^2}{\partial x^2}\mathscr{H}\{w\}\right) = 0, \tag{3.2a}$$

$$\int_0^h\int_{-b}^b w\,\mathrm{d}x\,\mathrm{d}z = Qt^\alpha. \tag{3.2b}$$

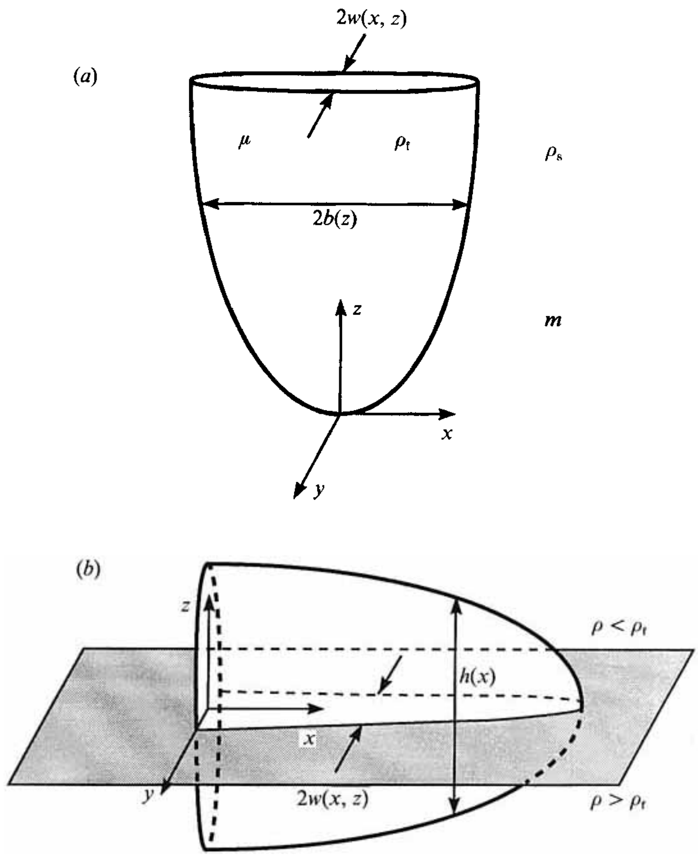

FIGURE 1. (a) A buoyant fluid of density ρ_f and viscosity μ rises through a crack in a solid of density ρ_s and elastic modulus $m = G/(1-\nu)$. (b) A fluid-filled crack propagates laterally in a stratified solid. The neutral-buoyancy level of the fluid forms the plane $z = 0$.

It is possible to find solutions of (3.2) in terms of the similarity variables ξ, ζ and W defined by

$$z = \left(\frac{(g\,\Delta\rho)^3\,Q^3 t^{3\alpha+2}}{m\mu^2}\right)^{\frac{1}{6}}\zeta, \tag{3.3a}$$

$$x = \left(\frac{mQt^{\alpha}}{g\,\Delta\rho}\right)^{\frac{1}{4}}\xi, \tag{3.3b}$$

$$w(x,z,t) = \left(\frac{\mu^4 Q^3 t^{3\alpha-4}}{m(g\,\Delta\rho)^3}\right)^{\frac{1}{12}} W(\xi,\zeta). \tag{3.3c}$$

Unfortunately, it is not clear what boundary conditions should be imposed at the edges of the crack $\xi = \xi_N(\zeta)$ for $0 < \zeta < \zeta_N$. At the downwards-facing edges we expect $W(\xi_N(\zeta),\zeta) = 0$. However, at the upwards-facing edges we expect to find a leading elastic shock wave analogous to that found at the leading edge of a two-dimensional crack (Lister 1990*a*). The boundary condition to be imposed on W would depend on the unknown details of the elastic shock and we are forced to conclude simply that the size of the crack is given by (3.3), where ξ and ζ have maximum values, ξ_N and ζ_N, of order unity.

We may make more progress in the important special case of fixed-flux release ($\alpha = 1$). After the initial crack-propagation front has passed, the shape of the crack and the flow will approach a steady state in which $\partial w/\partial t = 0$ and the flux through any cross-section is given by Q. Accordingly, we look for solutions of

$$g\,\Delta\rho\frac{\partial w^3}{\partial z}+m\frac{\partial}{\partial x}\left(w^3\frac{\partial^2}{\partial x^2}\mathscr{H}\{w\}\right)=0, \tag{3.4a}$$

$$\frac{2g\,\Delta\rho}{3\mu}\int_{-b(z)}^{b(z)} w^3\,\mathrm{d}x = Q. \tag{3.4b}$$

We solve these equations by defining similarity variables ξ and W, where

$$x = b_N\left(\frac{3Q\mu m^3z^3}{2(g\,\Delta\rho)^4}\right)^{\frac{1}{10}}\xi \tag{3.5a}$$

$$w(x,z) = b_N^3\left(\frac{27Q^3\mu^3}{8m(g\,\Delta\rho)^2z}\right)^{\frac{1}{10}}W(\xi), \tag{3.5b}$$

and where b_N is chosen so that $W(\pm 1) = 0$. In terms of the new variables, (3.4) become

$$(W^3(\mathscr{H}\{W\})'')' = \tfrac{3}{10}W^2(W+3\xi W'), \tag{3.6a}$$

$$b_N = \left(\int_{-1}^{1} W^3\,\mathrm{d}\xi\right)^{-\frac{1}{10}}. \tag{3.6b}$$

We integrate (3.6a) to obtain

$$W^3(\mathscr{H}\{W\})'' = \tfrac{3}{10}\xi W^3 + c_3, \tag{3.7}$$

where c_3 is the constant of integration. Use of the boundary condition $W(\pm 1) = 0$ shows that $c_3 = 0$. We divide by W^3 and integrate again to find that

$$\mathscr{H}\{W\}' = \tfrac{3}{20}\xi^2 + c_4, \tag{3.8}$$

where c_4 is another constant of integration. The Hilbert transform in (3.8) may be inverted by means of standard transforms (e.g. Erdelyi *et al.* 1954) or by substitution into (2.18c). The resultant solution,

$$W = -\left(\frac{2\xi^2+1}{40}+c_4\right)(1-\xi^2)^{\frac{1}{2}}, \tag{3.9}$$

has a dimensionless stress intensity of $-c_4-\frac{3}{40}$ at $\xi = \pm 1$. If we use (3.5) to transform back to dimensional variables then we find that, with a suitable choice of value for c_4, (3.9) gives the solution for a buoyant crack rising through a solid in which the critical stress-intensity factor K is proportional to $z^{-\frac{1}{4}}$.

As shown in §2, K is negligible in geophysical problems. Therefore, the relevant value for c_4 in (3.9) is $c_4 = -\frac{3}{40}$ for which the stress intensity at $\xi = \pm 1$ is zero. With this value

$$W = \tfrac{1}{20}(1-\xi^2)^{\frac{3}{2}}, \tag{3.10a}$$

$$b_{\mathrm{N}} = \left(\frac{2048000}{63\pi}\right)^{\frac{1}{10}} = 2.52048\ldots. \tag{3.10b}$$

The smooth closure of the crack at $\xi = \pm 1$ follows from the neglect of the resistance of the medium to fracture. At very large values of z, however, the cross-stream elastic pressures decrease sufficiently that the resistance to fracture can no longer be neglected and there is a transition in behaviour from (3.5) to (2.13). We solve for the regime in which the resistance to fracture is dominant by noting that a vertical crack with an elliptic cross-section satisfies the fluid and elastic equations exactly. Specifically, a fluid-filled crack with cross-section $x^2/b^2+y^2/w^2 = 1$ will be held open by a constant internal pressure

$$p_0 = \frac{mw}{l_0} \tag{3.11a}$$

(Muskhelishvili 1975), where $l_0 = b+(1-2\nu)/[2(1-\nu)]\,w$, and will contain a velocity distribution

$$u = \frac{\Delta\rho g b^2 w^2}{2\mu(b^2+w^2)}\left(1-\frac{x^2}{b^2}-\frac{y^2}{w^2}\right). \tag{3.11b}$$

We equate the volume flux to Q and the stress intensity $mw/l_0^{\frac{1}{2}}$ to K, make the approximation $w \ll b$ and deduce that

$$b = \left(\frac{4m^3\mu Q}{\pi K^3\,\Delta\rho g}\right)^{\frac{2}{5}}, \quad w = \left(\frac{4K^2\mu Q}{\pi m^2\,\Delta\rho g}\right)^{\frac{1}{5}}. \tag{3.12a, b}$$

If we assume that the transition from (3.5) to (3.12) occurs where the widths given by (3.12a) and (3.5a) are equal then we conclude that (3.5) and (3.10) hold when

$$z < \frac{1}{5\pi}\left(\frac{21}{32}\right)^{\frac{1}{3}}\frac{m^3Q\mu}{K^4}. \tag{3.13}$$

This condition is easily satisfied for geophysical parameters.

4. Lateral propagation of a crack filled with neutrally buoyant fluid

In the previous section we considered the vertical propagation of a fluid-filled crack through a uniform elastic solid of greater density than the fluid. We now analyse the lateral propagation of the crack for the case in which the solid is horizontally stratified in density and the crack has risen to the level at which the fluid is neutrally buoyant. The distribution of stresses in the walls of a fluid-filled crack is such that there is a strong tendency for the crack to extend in its own plane as a 'Type I' fracture (Pollard 1987). Accordingly, we expect the lateral propagation of the crack along the neutral-buoyancy level to continue in the vertical plane defined by the rising feeder crack rather than to change direction by 90° and form a horizontal sheet. Continued propagation in a near-vertical plane is in agreement with geological observations (Rubin & Pollard 1987).

After a sufficient length of time the horizontal extent of the laterally propagating crack will be much greater than the width of the conduit bringing fluid from depth. Thus we may idealize the feeder conduit as a point source of fluid which we take to be at the origin of coordinates such that the plane of neutral buoyancy is given by $z = 0$ (figure 1*b*). Let the lateral crack occupy $|y| < w(x,z,t)$ for $h_1(x,t) < z < h_u(x,t)$ and $-x_N(t) < x < x_N(t)$. (There is, of course, symmetry about $x = 0$.) At sufficiently large times we will have $x_N \gg h_1, h_u$ and, as usual, $h_1, h_u \gg w$. Therefore, the pressure in the fluid will be given by the sum of the hydrostatic value and a constant excess pressure; the width of the crack will be given by (2.17), where the Hilbert transform is taken with respect to z. We suppose that the crack is fed at such a rate that the volume of fluid in the region of the crack lying in $x > 0$ is given by Qt^{α}.

Motivated by the scalings discussed in §2, we suppose, also, that the resistance to fracture of the solid is very much less than the available hydrostatic stresses. Therefore, the excess pressure in the fluid and the values of h_1 and h_u will be related in such a way that the stress intensities at the upper and lower edges of the crack are both zero. If the excess pressure is too large then the stress intensities will be positive, the vertical extent of the crack will increase and the excess pressure will decrease. If the average level of the crack is too low relative to the neutral-buoyancy level then the stress intensity will be greater at the upper edge of the crack than the lower and the crack will rise. This adjustment may be thought of as the crack 'floating' at the neutral-buoyancy level, though it should not be confused with the usual Archimedean concept of floating in a stratified fluid. As will be shown, the ratio of the heights above and below the neutral-buoyancy level is different for a crack 'floating' in a solid and an object floating in a fluid. We note that the vertical motion required to attain a floating configuration takes place on a much shorter timescale than the subsequent lateral spread (Lister & Kerr 1989).

We consider below lateral propagation in two canonical cases of density stratification – a density step and a linear density gradient.

4.1. *Propagation at a density step*

Consider an infinite elastic solid of density ρ_u in $z > 0$ and density ρ_l in $z < 0$. We assume, for simplicity, that the shear modulus and Poisson's ratio of the solid in the two regions are equal; the following theory could be extended to include the case of unequal properties but the results would only be altered by changes in some of the numerical constants. Suppose that fluid of intermediate density ρ_f is introduced at the origin, causing a crack to form in the plane $y = 0$.

Let $h(x,t) = h_u - h_l$ be the total height of the crack and define

$$\theta = \frac{\rho_l - \rho_f}{\rho_l - \rho_u} \quad \text{and} \quad \bar{\theta} = \frac{\rho_f - \rho_u}{\rho_l - \rho_u} = 1 - \theta.$$

Thus the difference between the hydrostatic pressure in the fluid and in the solid is given by

$$p = p_0(x) - \bar{\theta}(\rho_l - \rho_u)gz \quad (0 < z < h_u), \tag{4.1a}$$

$$p = p_0(x) + \theta(\rho_l - \rho_u)gz \quad (h_l < z < 0), \tag{4.1b}$$

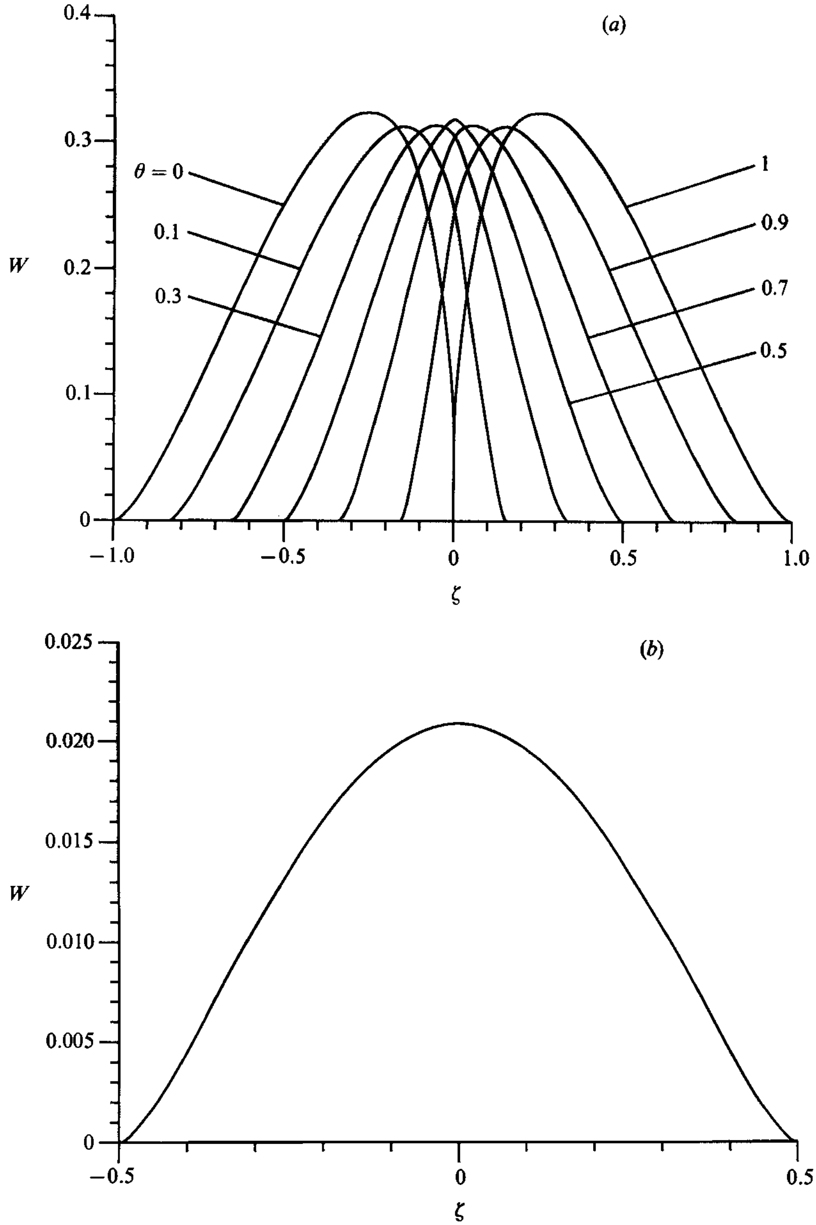

FIGURE 2. The dimensionless half-width W of a fluid-filled crack at the neutral-buoyancy level $\zeta = 0$ of the fluid in a stratified solid: (*a*) a crack at a density step, where $\theta = (\rho_1 - \rho_f)/(\rho_1 - \rho_u)$; (*b*) a crack in a linear density gradient.

where p_0 is the excess pressure in the fluid. The crack is held open by this pressure difference and its width may be calculated from (2.17). We define a dimensionless pressure P_0 and width W by

$$P_0 = \frac{p_0}{\theta\bar{\theta}(\rho_1 - \rho_u)\,gh}, \tag{4.2}$$

$$W = \frac{mw}{\theta\bar{\theta}(\rho_1 - \rho_u)\,gh^2}, \tag{4.3}$$

and let $\zeta = z/h$, $\zeta_l = h_l/h$ and $\zeta_u = h_u/h$. Thus W is the shape of a crack held open by a pressure $p = P_0 - \zeta/\theta$ for $0 < \zeta < \zeta_u$ and $p = P_0 + \zeta/\bar{\theta}$ for $\zeta_l < \zeta < 0$. The unknowns P_0, ζ_l, ζ_u and W are found by solving the problem consisting of equation (2.17), the equation $\zeta_u - \zeta_l = 1$ and the requirements of zero stress intensity at both edges of the crack. Since this problem is independent of x, the solutions depend only on the parameter θ: P_0, ζ_l and ζ_u are constants and W is a function of ζ. The details of the calculation of these constants and of $W(\zeta;\theta)$ are given in Appendix A; for the moment we take W to be a known function and focus our attention on the calculation of the variation of h with x. In figure 2(*a*) we show W for a few values of θ.

The lateral variations in the pressure given by (4.1) drive a flow in the crack. We integrate (2.16) with respect to z to deduce that

$$\frac{\partial}{\partial t}\int_{h_l}^{h_u} w\,\mathrm{d}z = \frac{1}{3\mu}\frac{\partial}{\partial x}\left(\frac{\partial p}{\partial x}\int_{h_l}^{h_u} w^3\,\mathrm{d}z\right). \tag{4.4}$$

Substitution from (4.1)–(4.3) leads to

$$I_1\frac{\partial h^3}{\partial t} = \frac{I_3 P_0(\theta\bar{\theta}(\rho_l-\rho_u)g)^3}{3\mu m^2}\frac{\partial}{\partial x}\left(h^7\frac{\partial h}{\partial x}\right), \tag{4.5a}$$

where $I_j(\theta) = 2\int_{\zeta_l}^{\zeta_u} W^j(\zeta)\,\mathrm{d}\zeta$. The problem is completed by the equation of global conservation of volume

$$\frac{I_1\theta\bar{\theta}(\rho_l-\rho_u)g}{m}\int_0^{x_N} h^3\,\mathrm{d}x = Qt^{\alpha}. \tag{4.5b}$$

While solutions of equations (4.5) may be obtained numerically from given initial conditions, it is better to observe that the problem has a similarity solution and that any solution with sufficiently smooth initial conditions will tend to this similarity form. We define similarity variables ξ and H by

$$x = \xi_N\left(\frac{I_3^3P_0^3(\theta\bar{\theta}(\rho_l-\rho_u)g)^4Q^5t^{5\alpha+3}}{27I_1^8\mu^3m}\right)^{\frac{1}{11}}\xi, \tag{4.6a}$$

$$h(x,t) = \xi_N^{\frac{2}{5}}\left(\frac{3\mu m^4Q^2t^{2\alpha-1}}{I_1I_3P_0(\theta\bar{\theta}(\rho_l-\rho_u)g)^5}\right)^{\frac{1}{11}}H(\xi), \tag{4.6b}$$

where ξ_N is chosen so that $H(1) = 0$. In terms of the new variables, (4.5) become

$$3H^2\left(\frac{2\alpha-1}{11}H - \frac{5\alpha+3}{11}\xi H'\right) = (H^7H')', \tag{4.7a}$$

$$\xi_N = \left(\int_0^1 H^3\,\mathrm{d}\xi\right)^{-\frac{5}{11}}. \tag{4.7b}$$

Using the boundary condition $H(1) = 0$, we find that around $\xi = 1$ the solution must satisfy

$$H = \left(\frac{5(5\alpha+3)(1-\xi)}{11}\right)^{\frac{1}{5}}\left(1+\frac{3}{80}\frac{5\alpha-8}{5\alpha+3}(1-\xi)+O(1-\xi)^2\right). \tag{4.8}$$

This asymptotic result may be used as a starting condition for inwards numerical integration of (4.7*a*). Solutions for H at various values of α and the dependence of the

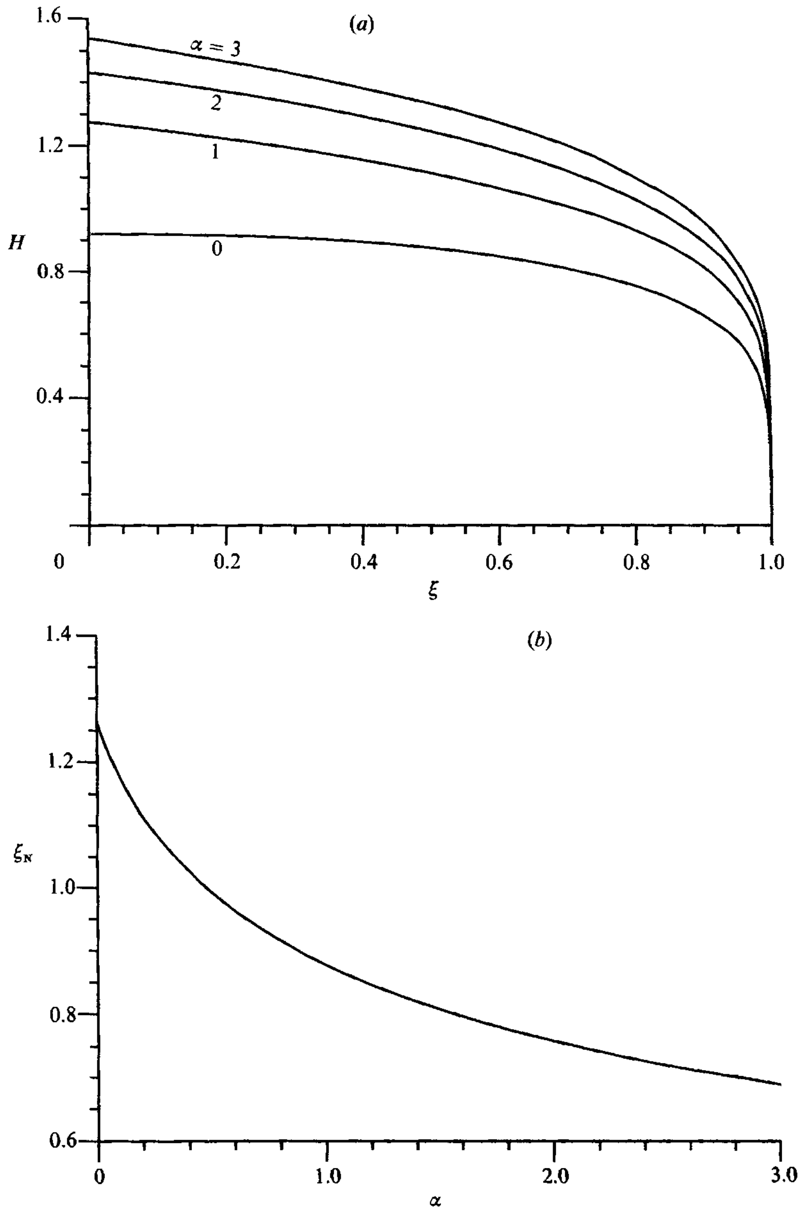

FIGURE 3. A crack of volume Qt^{α} propagating at a density step. (*a*) The height H of the crack as a function of lateral position ξ; (*b*) the dimensionless length ξ_N of the crack as a function of α.

constant ξ_N on α are shown in figure 3. In the interesting case of a fixed-volume release ($\alpha = 0$) we can integrate (4.7) analytically to obtain the exact solution

$$H = \left(\tfrac{15}{22}(1-\xi^2)\right)^{\frac{1}{5}}, \quad \xi_N = \left(\frac{11}{30}\right)^{\frac{3}{11}} \left(\frac{\Gamma(\frac{16}{5})}{\Gamma^2(\frac{8}{5})}\right)^{\frac{5}{11}} = 1.26009\ldots. \qquad (4.9a, b)$$

A further analytic solution may be obtained for the case $\alpha = \frac{8}{5}$:

$$H = (5(1-\xi))^{\frac{1}{5}}, \quad \xi_N = \frac{8^{\frac{5}{11}}}{5^{\frac{8}{11}}} = 0.798277\ldots. \qquad (4.10a, b)$$

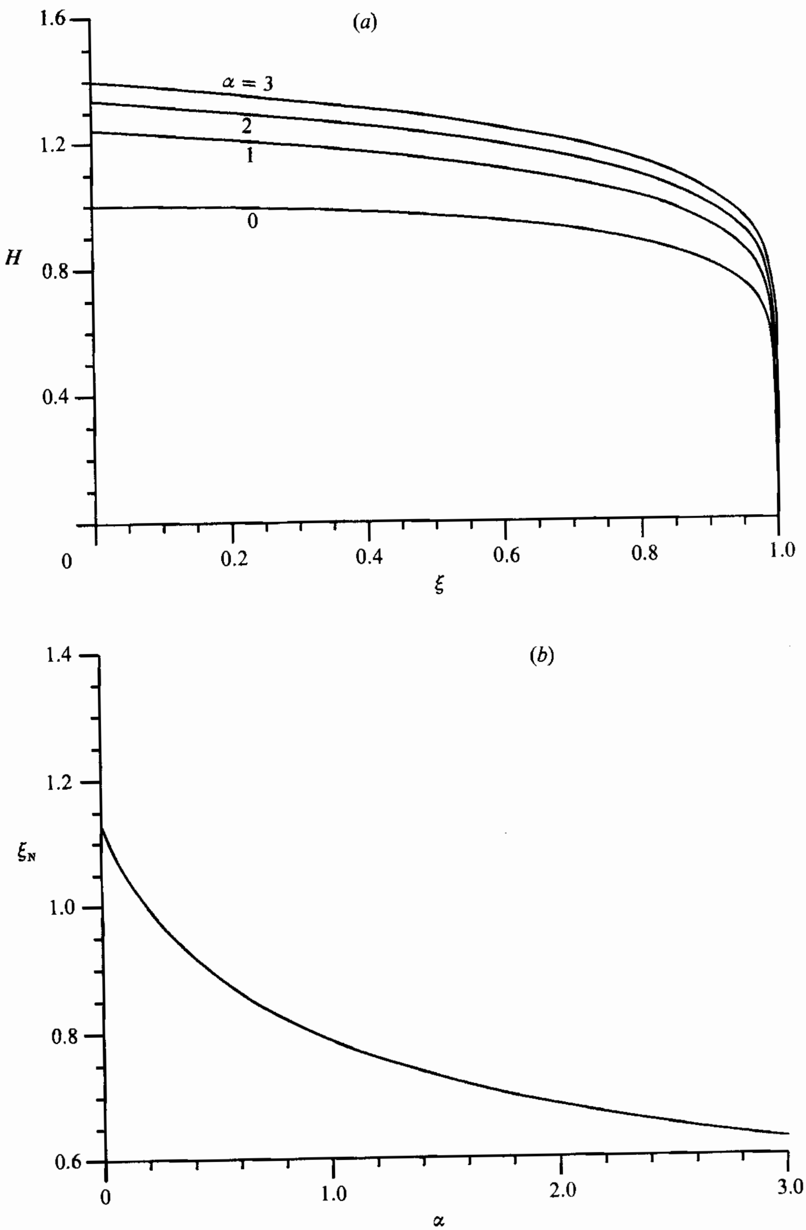

FIGURE 4. A crack of volume Qt^{α} propagating at a density gradient. (a) The height H of the crack as a function of lateral position ξ; (b) the dimensionless length ξ_N of the crack as a function of α.

4.2. *Propagation in a density gradient*

Now suppose that the fluid is released into a continuously stratified solid with density $\rho = \rho_f - Rz$. By symmetry, it is clear that the crack will 'float' with $h_u = -h_l = \frac{1}{2}h$. Hence, the difference between the hydrostatic pressure in the fluid and the solid is given by

$$p = p_0(x) - \tfrac{1}{2}Rgz^2 \quad (|z| < \tfrac{1}{2}h). \tag{4.11}$$

The pressure difference causes the crack to remain open with width given by

$$w = \frac{Rgh^3}{m} W(\zeta;\theta), \tag{4.12}$$

where $\zeta = z/h$, W is the dimensionless crack width corresponding to a pressure $p = P_0 - \frac{1}{2}\zeta^2$ for $|\zeta| < \frac{1}{2}$ and $P_0 = p_0/Rgh^2$. The function W and constant P_0 are independent of x and are calculated in Appendix A; the solution for W is shown in figure 2(*b*).

As in §4.1, the lateral variations in the fluid pressure drive a flow in the crack and the vertical cross-sectional area of the crack evolves according to (4.4) as the crack propagates. We substitute from (4.11) and (4.12) into (4.4) and into the equation of global conservation of volume. We find that h is governed by the equations

$$I_1 \frac{\partial h^4}{\partial t} = \frac{2I_3 P_0 R^3 g^3}{3\mu m^2} \frac{\partial}{\partial x}\left(h^{11}\frac{\partial h}{\partial x}\right), \tag{4.13a}$$

$$\frac{I_1 Rg}{m}\int_0^{x_N} h^4 \,\mathrm{d}x = Qt^{\alpha}. \tag{4.13b}$$

Equations (4.13) have a structure that resembles that of equations (4.5) and the analysis of the two sets of equations is very similar. Use of similarity variables defined by

$$x = \xi_N \left(\frac{2I_3 P_0 RgQ^2 t^{2\alpha+1}}{3I_1^3 \mu}\right)^{\frac{1}{4}} \xi, \tag{4.14a}$$

$$h(x,t) = \xi_N^{\frac{1}{4}} \left(\frac{3\mu m^4 Q^2 t^{2\alpha-1}}{2I_1 I_3 P_0 R^5 g^5}\right)^{\frac{1}{16}} H(\xi) \tag{4.14b}$$

gives rise to

$$H^3[\tfrac{1}{4}(2\alpha-1)H - (2\alpha+1)\xi H'] = (H^{11}H')', \tag{4.15a}$$

$$\xi_N = \left(\int_0^1 \phi^4 \,\mathrm{d}\xi\right)^{-\frac{1}{2}} \tag{4.15b}$$

with local solution

$$H = (2(2\alpha+1)(1-\xi))^{\frac{1}{8}}\left(1 + \frac{1}{48}\frac{2\alpha-3}{2\alpha+1}(1-\xi) + O(1-\xi)^2\right). \tag{4.16}$$

Numerical solutions of (4.15) are shown in figure 4. Once again, we can obtain exact solutions for certain values of α:

$$H = (1-\xi^2)^{\frac{1}{8}}, \quad \xi_N = \frac{2}{\pi^{\frac{1}{2}}} = 1.128379\ldots \quad (\alpha = 0), \tag{4.17a, b}$$

$$H = [8(1-\xi)]^{\frac{1}{8}}, \quad \xi_N = \left(\frac{9}{32}\right)^{\frac{1}{4}} = 0.728238\ldots \quad (\alpha = \tfrac{3}{2}). \tag{4.18a, b}$$

5. Turbulent flow in propagating cracks

In the previous sections we derived the equations governing the vertical and lateral propagation of a fluid-filled crack under the assumption that the flow is laminar. In the laminar regime the local volume flux is given by

$$\boldsymbol{q} = -\frac{2}{3\mu} w^3 \nabla p. \tag{5.1a}$$

If the Reynolds number $Re = \rho|\boldsymbol{q}|/\mu$ exceeds $O(10^3)$ then the flow in the crack will be turbulent and the flux should be related to the pressure gradient and the width of the crack by an appropriate empirical flow law rather than by (5.1a). A commonly used and simple flow law is

$$\boldsymbol{q} = -\left(\frac{8}{k\rho_{\mathrm{f}}|\nabla p|}\right)^{\frac{1}{2}} w^{\frac{3}{2}}\nabla p, \tag{5.1b}$$

where the friction factor k has a constant value of about 0.03, depending somewhat on the surface roughness of the crack (Huppert *et al.* 1984). Theoretical arguments (Schlichting 1968) suggest that k also varies with Reynolds number like $Re^{\frac{1}{4}}$. Substituting into (5.1b) we find that

$$\boldsymbol{q} = -\frac{15.4}{(\mu\rho_{\mathrm{f}}^3|\nabla p|^3)^{\frac{1}{7}}} w^{\frac{12}{7}}\nabla p, \tag{5.1c}$$

where the numerical coefficient has been determined experimentally (Hirs 1974).

The flow laws (5.1a–c) have sufficiently similar structures that the analysis of laminar flows in §§3 and 4 may be extended to turbulent flows. Below we give an outline of the analysis for both vertically and laterally propagating cracks in the turbulent regime. It should be noted that the flow will necessarily be laminar close to the edges of a propagating crack owing to the small crack widths there. We assume, however, that the shape and propagation rate are determined globally by the turbulent flow in the major part of the crack.

5.1. *Turbulent, vertical flow*

As in §3, we consider the upwards propagation of a crack containing buoyant fluid. The fluid velocity is nearly vertical and the vertical pressure gradient in the fluid is much greater than the horizontal gradient. From (3.1), therefore, we make the approximation that $|\nabla p| = g\,\Delta\rho$. In consequence, (5.1) may be written in the form

$$\boldsymbol{q} = -Aw^a\nabla p, \tag{5.2}$$

where a and A are constants which depend on the flow regime. The resultant equations for steady flow

$$\Delta\rho g\frac{\partial w^a}{\partial z} + m\frac{\partial}{\partial x}\left(w^a\frac{\partial^2}{\partial x^2}\mathscr{H}\{w\}\right) = 0, \tag{5.3a}$$

$$A\,\Delta\rho g\int_{-b(z)}^{b(z)} w^a\,\mathrm{d}x = Q \tag{5.3b}$$

have a solution

$$w(x,z) = \frac{ab_{\mathrm{N}}^3}{6(3a+1)}\left(\frac{Q^3}{A^3(g\,\Delta\rho)^2\,mz}\right)^{1/(3a+1)}(1-\xi^2)^{\frac{3}{2}}, \tag{5.4a}$$

where
$$\xi = \frac{x}{b_{\mathrm{N}}}\left(\frac{Qm^az^a}{A(g\,\Delta\rho)^{a+1}}\right)^{-1/(3a+1)} \tag{5.4b}$$

$$b_{\mathrm{N}} = \frac{1}{2}\left(\frac{6(3a+1)}{a}\right)^{a/(3a+1)}\left(\frac{\Gamma(3a+2)}{\Gamma^2(\frac{1}{2}(3a+2))}\right)^{1/(3a+1)}. \tag{5.4c}$$

The values of a and A and the dependence of w and b on z for the different flow regimes are summarized in table 1.

Flow regime	a	A	w	b
Laminar (5.1*a*)	3	$2/3\,\mu$	$\propto z^{-\frac{1}{10}}$	$\propto z^{\frac{3}{10}}$
Turbulent (5.1*b*)	$\frac{3}{2}$	$(8/k\rho_f g\,\Delta\rho)^{\frac{1}{2}}$	$\propto z^{-\frac{2}{11}}$	$\propto z^{\frac{3}{11}}$
Turbulent (5.1*c*)	$\frac{12}{7}$	$15.4\mu^{-\frac{1}{7}}(\rho_f g\Delta\rho)^{-\frac{3}{7}}$	$\propto z^{-\frac{7}{43}}$	$\propto z^{\frac{12}{43}}$

TABLE 1. Vertical flow in a buoyant crack

	Flow regime	a	A'	c	x_N	h
(*a*)	Laminar (5.1*a*)	3	$1/3\,\mu$	1	$\propto t^{(5\alpha+3)/11}$	$\propto t^{(2\alpha-1)/11}$
	Turbulent (5.1*b*)	$\frac{3}{2}$	$(2/k\rho_f)^{\frac{1}{2}}$	$\frac{1}{2}$	$\propto t^{(\alpha+2)/4}$	$\propto t^{(3\alpha-2)/12}$
	Turbulent (5.1*c*)	$\frac{12}{7}$	$7.7\mu^{-\frac{1}{7}}\rho_f^{-\frac{3}{7}}$	$\frac{4}{7}$	$\propto t^{7(2\alpha+3)/47}$	$\propto t^{(11\alpha-7)/47}$
(*b*)	Laminar (5.1*a*)	3	$1/3\,\mu$	1	$\propto t^{(2\alpha+1)/4}$	$\propto t^{(2\alpha-1)/16}$
	Turbulent (5.1*b*)	$\frac{3}{2}$	$(2/k\rho_f)^{\frac{1}{2}}$	$\frac{1}{2}$	$\propto t^{(5\alpha+8)/17}$	$\propto t^{(3\alpha-2)/17}$
	Turbulent (5.1*c*)	$\frac{12}{7}$	$7.7\mu^{-\frac{1}{7}}\rho_f^{-\frac{3}{7}}$	$\frac{4}{7}$	$\propto t^{(23\alpha+28)/67}$	$\propto t^{(11\alpha-7)/67}$

TABLE 2. (*a*) Lateral flow at a density step, (*b*) lateral flow in a density gradient

5.2. *Turbulent lateral flow*

Consider the lateral propagation of a crack that contains fluid at its neutral-buoyancy level. The driving pressure in the fluid is given by (4.1) and (4.11) for the cases of a density step and a density gradient respectively. The lateral pressure gradient and the width of the crack may be put in the form

$$\frac{\partial p}{\partial x} = B\frac{\partial h^b}{\partial x}, \quad w = \frac{Bh^{b+1}}{m}W(\zeta), \tag{5.5a, b}$$

where $B = P_0\,\theta\bar{\theta}(\rho_l-\rho_u)\,g$ and $b = 1$ for a density step or $B = \frac{1}{8}P_0 Rg$ and $b = 2$ for a density gradient. The flux laws (5.1) may be written in the form

$$\boldsymbol{q} = 2A'w^a\boldsymbol{\nabla}p^c, \tag{5.5c}$$

where we take $\boldsymbol{\nabla}p^c$ to mean $|\boldsymbol{\nabla}p|^{c-1}\boldsymbol{\nabla}p$ and A', a and c are constants as given in table 2. We substitute (5.5) into the depth-integrated equation of continuity and the equation for the volume of the crack to find that

$$\frac{\partial h^{b+2}}{\partial t} = \frac{I_a A'B^{a+c-1}b^c}{I_1 m^{a-1}}\frac{\partial}{\partial x}\left\{h^{a(b+1)+c(b-1)+1}\left(\frac{\partial h}{\partial x}\right)^c\right\}, \tag{5.6a}$$

$$\frac{BI_1}{m}\int_0^{x_N} h^{b+2}\,\mathrm{d}x = Qt^\alpha. \tag{5.6b}$$

Similarity solutions of these equations are derived in Appendix B. Further, it is shown therein that equations with the same mathematical structure as (5.6) may also be used to describe the spread of viscous gravity currents on a rigid surface (Huppert 1982*a*), over a fluid layer (Lister & Kerr 1989) and in a porous medium or Hele-Shaw cell. Here, however, we note simply that h and x_N each vary as powers of t and summarize in table 2 the power laws for the different flow regimes and for propagation at a density step and a density interface.

6. Discussion

Our analysis of the magnitude of the pressures involved in the propagation of fluid-filled cracks has identified the parameter regimes in which different physical balances characterize the flow. For the geophysical parameters relevant to dyke propagation, we have shown that the resistance of the rock to fracture only plays a role during the nucleation of a new crack. Thereafter, the dominant resistance to further fracture is provided by the viscous pressure drop in the melt as it flows towards the crack tip. The motion is driven by elastic stresses if the crack is of small vertical extent, as defined by (2.11), or, more commonly, by buoyancy forces arising from the difference in density between the melt and the surrounding rock. The conclusion follows that magma will rise from the base of the lithosphere through vertical dykes, driven by its buoyancy. If the uppermost layers of the lithosphere are less dense then the magma will tend to be emplaced in dykes which propagate laterally at the neutral-buoyancy level of the melt.

Analytic solutions have been derived to model each of the vertical and lateral stages of magma transport in both the laminar and turbulent regimes. These solutions describe the shape, dimensions and rate of propagation of a fluid-filled crack and provide models which give qualitative and quantitative insight into the mechanics of dyke emplacement. In order to focus on the important physical features of crack propagation in these geometries, we have made a number of simplifying assumptions in the analysis which should now be discussed.

We note, first, that we assumed that the downstream extent of the crack is much greater than the cross-stream extent. It is clear that this will indeed be the case at sufficiently large times; the transition time (or length) at which the assumption becomes valid may easily be determined by equating (3.3*a*) and (3.3*b*), (4.6*a*) and (4.6*b*) or (4.14*a*) and (4.14*b*), as appropriate. The conditions giving the times for which the width of the crack w is much smaller than either extent may be evaluated in a similar way, though these conditions are not at all restrictive for geophysical parameters.

Secondly, the details of the shape of a laterally propagating crack will depart from the similarity form within an $O(h)$ neighbourhood of the nose at $x = x_{\mathrm{N}}(t)$. These departures will be due to the local breakdown of the assumption $\partial h/\partial x \ll 1$, which is required in order that (2.17) describe the vertical cross-section of the crack, and to a small volume of inviscid volatiles in the extreme tip of the crack, which are exsolved in the tip of any extending fluid-filled fracture (Lister 1990*a*). However, these effects are confined to a small neighbourhood of the nose of the crack and do not influence the global dynamics of the flow, which determine the shape and propagation rate of the crack (cf. similar discussion in Huppert 1982*a* and Lister & Kerr 1989).

Thirdly, in application of the emplacement of dykes, our solutions of the equations of fluid motion and elastic deformation may need to be coupled to the thermal problem of heat transfer from the magma to the colder country rock. Both solidification and melting are possible (Bruce & Huppert 1989, 1990), with soldification most important in the narrow dyke tips and meltback enhanced by turbulent flow. Detailed inclusion of thermal effects must be deferred for future research and we note simply the conclusion that dykes in which solidification or melting is significant will have a greater width and smaller cross-stream extent than the values predicted here. The dominant pressure balances, however, will be as described and our solutions provide a bound or estimate for the dimensions of actual dykes. It is of interest, therefore, to evaluate our solutions for geological parameters.

We take as typical values for the material properties $G = 2\times10^{10}$ Pa, $\nu = 0.25$, $\mu = 100$ Pa s^{-1} and $\rho_f = 2600$ kg m^{-3} (see Lister 1990*a*). We assume that a density $\rho_l = 2900$ kg m^{-3} is typical for the lithosphere at depth and that there is a shallow, surface layer of density $\rho_u = 2300$ kg m^{-3} (Rubin & Pollard 1987). From (3.5) and (3.10) we calculate that a vertical dyke carrying a flux $Q = 100$ m^3 s^{-1} through the lithosphere would have a horizontal extent $2b = 18$ km and a width $2w$ of only 18 cm at a height of 50 km above the reservoir that feeds the base of the dyke. A large flux $Q = 10^6$ m^3 s^{-1}, such as is appropriate to eruptions of flood basalts (Swanson *et al.* 1975), gives a width of 2.8 m and horizontal extent of 46 km. These calculations, particularly for the smaller volume flux, predict dykes that are narrower and of greater horizontal extent that seems possible for the transport of melt through cold lithosphere. As discussed in §2, the resistance of the lithosphere to fracture is too small to have any significant effect on the lateral extent of the dyke. We conclude, therefore, that solidification at the edges of the dyke and thermal erosion at its centre are likely to limit the extent of the flow and concentrate it into a wider dyke that would be capable of transporting the melt without further solidification. We now consider the lateral emplacement of dykes at the neutral-buoyancy level of the melt. An intrusive event lasting for 2×10^5 s with $Q = 500$ m^3 s^{-1} is predicted by (4.3) and (4.6) to have length $x_N = 18$ km, width 1.2 m and average height 5 km. A smaller event with $t = 10^5$ s and $Q = 250$ m^3 s^{-1} gives $x_N = 8$ km, a width of 80 cm and a height of 4 km. These values are in agreement with observations of dykes intruded laterally beneath the summit of Kilauea Volcano, Hawaii (Ryan 1987). In the case of lateral intrusion, it would seem that the stratification in the country rock ensures that the dyke is sufficiently concentrated near the neutral-buoyancy level for thermal effects not to dominate the shape and propagation of the dyke.

We turn from the application of our results to their relation to previous studies of fluid fracture and of viscous gravity currents. The axisymmetric solution of Spence & Sharp (1985) and those given here form a geometrically complete set which represent the three canonical possibilities for the propagation of a fluid-filled crack from a point source. As shown in figure 5, these possibilities are the horizontal propagation of a crack lying in a horizontal plane (Spence & Sharp 1985), the vertical propagation of a crack in a vertical plane (§3) and the horizontal propagation of a crack lying in a vertical plane (§4).

Interesting parallels exist between these three solutions and solutions for viscous gravity currents over a horizontal plane (Huppert 1982*a*), down a sloping plane (Smith 1973) and at an interface (Lister & Kerr 1989). The dominant downstream balance between buoyancy forces and the viscous pressure drop in a thin layer is common to all these problems. Analogies may be drawn between the elastic shock at the tip of a propagating crack and the surface-tension-dominated region (Huppert 1982*b*) at the front of a gravity current, between the critical stress-intensity at which a crack-tip will propagate and the critical contact angle at which a contact-line will move and between cross-stream spreading due either to elastic or to hydrostatic pressures caused by variations in the thickness of the flow. Such analogies are, of course, qualitative rather than quantitative but they are useful aids when considering the behaviour of propagating cracks.

To sum up, in this paper we have analysed the balance of forces in a propagating fluid-filled crack and derived solutions to the governing equations in two model

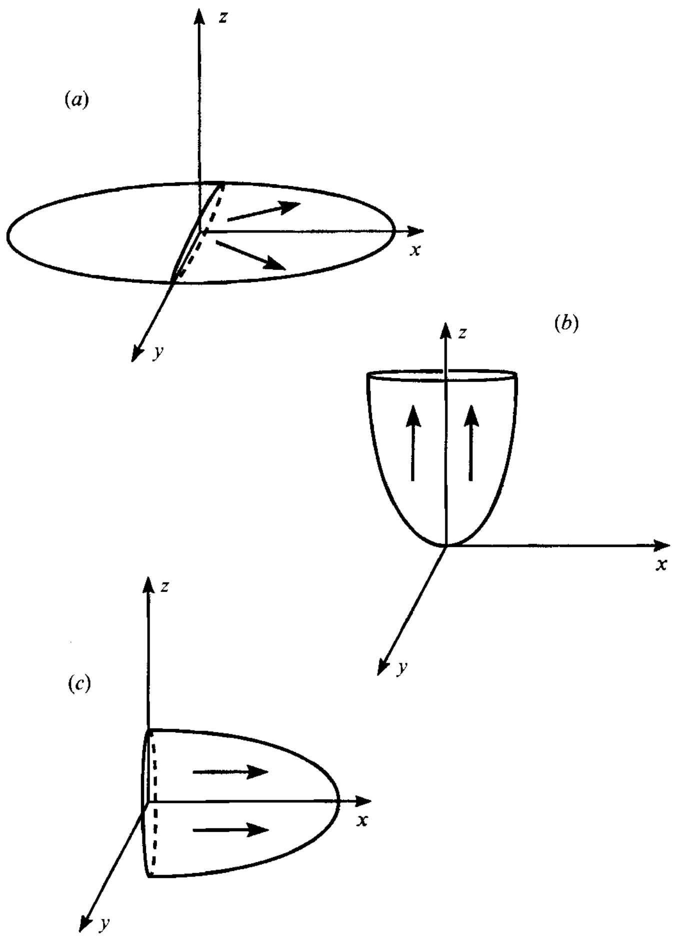

FIGURE 5. The three geometrical possibilities for propagation of a fluid-filled crack from a point source: (a) horizontal propagation in a horizontal plane – non-buoyant fluid; (b) vertical propagation in a vertical plane – buoyant fluid; (c) horizontal propagation in a vertical plane – neutrally buoyant fluid in a stratified solid.

geometries. These solutions increase our understanding of the dynamics of dyke emplacement and igneous intrusion and, hence, of the formation of many of the world's important mineral deposits.

Appendix A. The cross-section W of a laterally propagating crack

In §4 we wished to know the width $W(\zeta;\theta)$ of a crack occupying $\zeta_l < \zeta < \zeta_u$ and held open by a given pressure distribution. For convenience of notation, we define $s = 2\zeta + s_0$, where $s_0 = -2\zeta_l - 1$, so that $W(s)$ is the width of a crack held open either by the pressure

$$p = \tfrac{1}{2}P_0 + \frac{s_0 - s}{2\theta} \qquad (s_0 < s < 1), \tag{A 1a}$$

$$p = \tfrac{1}{2}P_0 + \frac{s - s_0}{2\theta} \qquad (-1 < s < s_0) \tag{A 1b}$$

relevant to §4.1, or by the pressure

$$p = \tfrac{1}{16}(8P_0 - s^2) \quad (-1 < s < 1) \tag{A 2}$$

relevant to §4.2. The crack is finite in extent and so W' and p are related by (2.18*c*), where $s_* = 1$ and $m = 1$.

The constants P_0 and s_0 in (A 1) are determined by the requirements that the stress intensities $K_\pm$ at $s = \pm 1$ are both zero. From (2.17) and equation (28) of Erdelyi *et al.* (1954, p. 249) we find that $K_\pm = \pm \lim_{s \to \pm 1}[W'(1-s^2)^{\frac{1}{2}}]$. Expansion of (2.18*c*) about $s = \pm 1$ then shows that

$$K_\pm = \frac{1}{\pi}\int_{-1}^{1} p(s)\left(\frac{1 \pm s}{1 \mp s}\right)^{\frac{1}{2}} \mathrm{d}s. \tag{A 3}$$

We substitute from (A 1), impose $K_\pm = 0$ and obtain equations for P_0 and s_0:

$$\cos^{-1} s_0 - s_0(1-s_0^2)^{\frac{1}{2}} = \pi\theta, \quad P_0 = \frac{(1-s_0^2)^{\frac{3}{2}}}{\pi\theta\bar{\theta}}. \tag{A 4a, b}$$

The solutions of these equations are shown as functions of θ in figure 6(*a*, *b*). The crack may be thought of as 'floating' at the neutral-buoyancy level with the density step at $s = s_0$. We note that, except for $\theta = 0$, $\frac{1}{2}$ and 1, this differs from the usual Archimedean concept of floating in a fluid which, for a flat object of uniform thickness, gives $s_0 = 1 - 2\theta$.

Having found s_0 and P_0, we now solve for W. We integrate (2.18*c*) with respect to s to obtain

$$W(s) = \frac{1}{\pi}\int_{-1}^{1} p(\sigma) \ln\left|\frac{1-\sigma s + [(1-\sigma^2)(1-s^2)]^{\frac{1}{2}}}{\sigma - s}\right| \mathrm{d}\sigma. \tag{A 5}$$

Since p is piecewise linear in (A 1), we integrate (A 5) twice by parts and use $p'' = 0$. We find that

$$W(s) = \frac{1}{\pi}\left(\frac{\mathscr{K}(1;s) - \mathscr{K}(s_0;s)}{2\theta} + \frac{\mathscr{K}(-1;s) - \mathscr{K}(s_0;s)}{2\bar{\theta}} + p(1)\,\mathscr{J}(1;s) - p(-1)\,\mathscr{J}(-1;s)\right), \tag{A 6a}$$

where

$$\begin{aligned}\mathscr{J}(\sigma;s) &= \int_s^{\sigma} \ln\left|\frac{1-\sigma' s + [(1-\sigma'^2)(1-s^2)]^{\frac{1}{2}}}{\sigma' - s}\right| \mathrm{d}\sigma' \\ &= (\sigma - s)\ln\left|\frac{1-\sigma s + [(1-\sigma^2)(1-s^2)]^{\frac{1}{2}}}{\sigma - s}\right| + (1-s^2)^{\frac{1}{2}}(\sin^{-1}\sigma - \sin^{-1} s),\end{aligned} \tag{A 6b}$$

$$\begin{aligned}\mathscr{K}(\sigma;s) &= \int_s^{\sigma}\int_s^{\sigma'} \ln\left|\frac{1-\sigma'' s + [(1-\sigma''^2)(1-s^2)]^{\frac{1}{2}}}{\sigma'' - s}\right| \mathrm{d}\sigma''\,\mathrm{d}\sigma' \\ &= \tfrac{1}{2}(\sigma - s)^2 \ln\left|\frac{1-\sigma s + [(1-\sigma^2)(1-s^2)]^{\frac{1}{2}}}{\sigma - s}\right| \\ &\quad + \tfrac{1}{2}(1-s^2)^{\frac{1}{2}}[(1-\sigma^2)^{\frac{1}{2}} - (1-s^2)^{\frac{1}{2}} + (2\sigma - s)(\sin^{-1}\sigma - \sin^{-1} s)].\end{aligned} \tag{A 6c}$$

The function $W(\zeta;\theta)$ is shown in figure 2(*a*) for a few values of θ. Except for the case $\theta = \frac{1}{2}$, the crack is asymmetrical about both the midline $s = 0$ and the neutral-buoyancy level $\zeta = 0$.

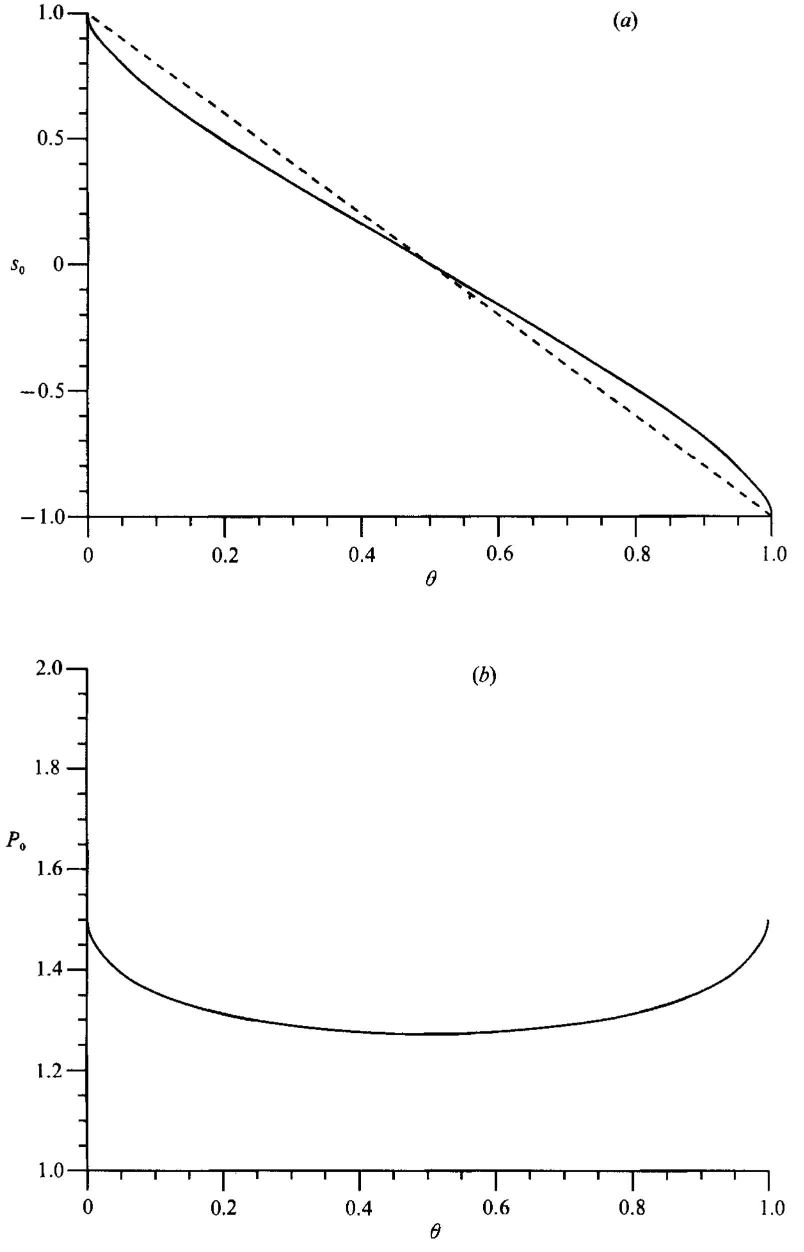

FIGURE 6. (*a*) The level s_0 of the neutral-buoyancy level for a crack 'floating' at a density interface as a function of $\theta = (\rho_l - \rho_f)/(\rho_l - \rho_u)$ (solid line). An object of uniform thickness would float in a fluid, in the usual Archimedean sense, with $s_0 = 1 - 2\theta$ (dashed line). (*b*) The excess pressure P_0 as a function of $\theta = (\rho_l - \rho_f)/(\rho_l - \rho_u)$.

To evaluate W due to the pressure distribution given by (A 2) we can either integrate (A 5) by parts a third time or invert (2.17) directly using standard Hilbert transform pairs (Erdelyi *et al.* 1954, p. 243 *et seq.*). We obtain

$$W(s) = \tfrac{1}{16}(8P_0 - \tfrac{1}{6} - \tfrac{1}{3}\sigma^3)(1 - s^2)^{\frac{1}{2}}. \tag{A 7}$$

If the stress intensity is to be zero at $s = \pm 1$ then $P_0 = \frac{1}{16}$. Hence the width of the crack is given by

$$W(s) = \tfrac{1}{48}(1-s^2)^{\frac{3}{2}} \tag{A 8}$$

as shown in figure 2(*b*).

Appendix B. General similarity theory for buoyancy-driven flows

Consider a two-dimensional flow of height $h(x,t)$ and horizontal extent $0 \leqslant x \leqslant x_N(t)$. Let the flow be driven by a pressure gradient that depends only on h and $\partial h/\partial x$ and which arises from a difference in density between the fluid and its surroundings. Suppose that the volume of the flow is proportional to t^α and that the geometry is such that the cross-sectional area is proportional to h^e for some constant e. We assume that the geometry and flow regime are such that the flux through a cross-section is proportional to $h^{d+e-c}(\partial h/\partial x)^c$, where c and d are constants and h'^c is taken to mean $|h'|^{c-1}h'$. Then consideration of local and global conservation of volume shows that

$$\frac{\partial h^e}{\partial t} = D\frac{\partial}{\partial x}\left\{h^{d+e-c}\left(\frac{\partial h}{\partial x}\right)^c\right\}, \quad \int_0^{x_N} h^e\,\mathrm{d}x = Et^\alpha, \tag{B 1a,b}$$

where D and E are constants. Similarity solutions to these equations may be found in terms of the variables ξ and $H(\xi)$, where

$$x = \xi_N((Dt)^e(Et^\alpha)^d)^{1/f}\xi, \quad h(x,t) = \xi_N^{(c+1)/d}((Et^\alpha)^{c+1}/(Dt))^{1/f}H(\xi), \tag{B 2a,b}$$

$f = ce+d+e$ and ξ_N is chosen so $H(1) = 0$. We substitute into (B 1) to obtain

$$\alpha H^e - \frac{d\alpha+e}{f}(\xi H^e)' = (H^{d+e-c}H'^c)', \quad \xi_N = \left(\int_0^1 H^e\,\mathrm{d}\xi\right)^{-d/f}. \tag{B 3a,b}$$

Analytic solutions may be found for particular values of α:

$$H = \left(\frac{e}{f}\right)^{1/d}\left(\frac{d}{c+1}(1-\xi^{(c+1)/c})\right)^{c/d}, \quad \xi_N = \left(\frac{(c+1)^{c+d}f}{c^d d^c e}\right)^{1/f}\mathrm{B}\left(\frac{c}{c+1},\frac{f-e}{d}\right)^{-d/f} \quad (\alpha = 0) \tag{B 4a,b}$$

$$H = \left(\frac{d}{c}(1-\xi)\right)^{c/d}, \quad \xi_N = \left(\frac{c^{ce}(f-e)^d}{d^{f-e}}\right)^{1/f} \quad (\alpha = (f-e)/d). \tag{B 5a,b}$$

In general, however, we need to integrate (B 3*a*) numerically from the asymptotic result

$$H \sim \left(\frac{d\alpha+e}{f}\right)^{1/d}\left(\frac{d(1-\xi)}{c}\right)^{c/d}\left(1+\frac{ce}{(f-e)(c+d+cd-c^2)}\frac{(d\alpha+e-f)}{(d\alpha+e)}(1-\xi)\right) \quad (\xi \to 1_-). \tag{B 6}$$

Equations (B 1)–(B 6) are applicable to a variety of fluid-mechanical problems. As described in §§4 and 5, the lateral propagation of a fluid-filled crack at a density step ($e = 3$) or in a density gradient ($e = 4$) is included in both the laminar ($c = 1$) and turbulent ($c = \frac{1}{2}$ or $c = \frac{4}{7}$) regimes. The spread of a viscous gravity current over a horizontal rigid surface is given by (B 1) with $c = 1$, $d = 3$ and $e = 1$ (Huppert

1982*a*); spread over a shallow layer of fluid is described by (B 1) with $c = 1$, $d = 2$ and $e = 1$ (Lister & Kerr 1989).

To our knowledge, solutions have not been published for the spread of a gravity current in a porous medium bounded below by a horizontal impermeable boundary or for a gravity current at the bottom edge of a vertical Hele-Shaw cell. It is easily shown that these problems are also included in the formalism above with $c = 1$, $d = 1$ and $e = 1$. The constant D is given by $D = l^2 g\,\Delta\rho/\mu$, where l^2 is given either by the permeability of the porous medium or by one sixth of the squared gap-width in the cell; E is simply the proportionality constant for the input volume.

Further applications of (B 1)–(B 6) arise in exotic situations such as intrusion into environments with an ambient density that varies according to a power law with height, or flow in Hele-Shaw cells with a gap width that varies according to a power law with height.

REFERENCES

AKI, K., FEHLER, M. & DAS, S. 1977 Source mechanisms of volcanic tremor: fluid-driven crack models and their application to the 1963 Kilauea eruption. *J. Volcanol. Geotherm. Res.* **2**, 259–287.

ANDERSON, O. L. & GREW, P. C. 1977 Stress corrosion theory of crack propagation with applications to geophysics. *Rev. Geophys. Space Phys.* **15**, 77–103.

BRUCE, P. M. & HUPPERT, H. E. 1989 Thermal controls of basaltic fissure eruptions. *Nature* **342**, 665–667.

BRUCE, P. M. & HUPPERT, H. E. 1990 Solidification and melting in dykes by the laminar flow of basaltic magma. In *Magma Transport and Storage* (ed. M. P. Ryan). Wiley.

CARMICHAEL, I. S. E., NICHOLLS, J., SPERA, F. J., WOOD, B. J. & NELSON, S. A. 1977 High temperature properties of silicate liquids: applications to the equilibration and ascent of basic magma. *Phil. Trans. R. Soc. Lond.* A **286**, 373–431.

ERDELYI, A., MAGNUS, W., OBERHETTINGER, F. & TRICOMI, F. G. (eds.) 1954 *Tables of Integral Transforms*. McGraw Hill.

FISKE, R. S. & JACKSON, E. D. 1972 Orientation and growth of Hawaiian volcanic rifts: the effect of regional structure and gravitational stresses. *Proc. R. Soc. Lond.* A **329**, 299–326.

HIRS, G. G. 1974 A systematic study of turbulent film flow. *J. Lubric. Tech.* **96**, 118–126.

HUPPERT, H. E. 1982*a* The propagation of two-dimensional and axisymmetric viscous gravity currents over a rigid horizontal surface. *J. Fluid Mech.* **121**, 43–58.

HUPPERT, H. E. 1982*b* Flow and instability of a viscous current down a slope. *Nature* **300**, 427–429.

HUPPERT, H. E. & SPARKS, R. S. J. 1985 Cooling and contamination of mafic and ultramafic magma during ascent through continental crust. *Earth Planet. Sci. Lett.* **74**, 371–386.

HUPPERT, H. E., SPARKS, R. S. J., TURNER, J. S. & ARNDT, N. T. 1984 Emplacement and cooling of komatiite lavas. *Nature* **309**, 19–22.

IRWIN, G. R. 1958 Fracture. In *Handbuch der Physics VI* (ed. S. Flügge), pp. 551–590. Springer.

LISTER, J. R. 1990*a* Buoyancy-driven fluid fracture: the effects of material toughness and of low-viscosity precursors. *J. Fluid Mech.* **210**, 263–280.

LISTER, J. R. 1990*b* Fluid-mechanical models of crack propagation and their application to magma-transport in dykes. *J. Geophys. Res.* (in preparation).

LISTER, J. R. & KERR, R. C. 1989 The propagation of two-dimensional and axisymmetric viscous gravity currents at a fluid interface. *J. Fluid Mech.* **203**, 215–249.

MAALOE, S. 1987 The generation and shape of feeder dykes from mantle sources. *Contrib. Min. Petrol.* **96**, 47–55.

MACDONALD, R., WILSON, L., THORPE, R. S. & MARTIN, A. 1988 Emplacement of the Cleveland Dyke: evidence from geochemistry, mineralogy and physical modelling. *J. Petrol.* **29**, 559–583.

MUSKHELISHVILI, N. I. 1975 *Some Basic Problems of the Mathematical Theory of Elasticity.* Noordhoff.

PASTERIS, J. D. 1984 Kimberlites: complex mantle salts. *Ann. Rev. Earth Planet. Sci.* **12**, 133–153.

POLLARD, D. D. 1987 Elementary fracture mechanics applied to the structural interpretation of dykes. In *Mafic Dyke Swarms* (ed. H. C. Halls & W. H. Fahrig). *Geol. Soc. Canada Special Paper* 34.

POLLARD, D. D. & HOLZHAUSEN, G. 1979 On the mechanical interaction between a fluid-filled fracture and the Earth's surface. *Tectonophys.* **53**, 27–57.

POLLARD, D. D. & MULLER, O. H. 1976 The effects of gradients in regional stress and magma pressure on the form of sheet intrusions in cross-section. *J. Geophys. Res.* **91**, 975–984.

RECHES, Z. & FINK, J. 1988 The mechanism of intrusion of the Inyo Dike, Long Valley Caldera, California. *J. Geophys. Res.* **93**, 4321–4334.

RUBIN, A. M. & POLLARD, D. D. 1987 Origins of blade-like dikes in volcanic rift zones. *US Geol. Survey Professional Paper* 1350.

RYAN, M. P. 1987 Neutral buoyancy and the mechanical evolution of magmatic systems. In *Magmatic Processes: Physicochemical Principles* (ed. B. O. Mysen), pp. 259–287. *Geochem. Soc. Special Publication* 1.

SCHLICHTING, H. 1968 *Boundary-Layer Theory.* McGraw-Hill.

SHAW, H. R. 1980 The fracture mechanisms of magma transport from the mantle to the surface. In *Physics of Magmatic Processes* (ed. R. B. Hargreaves), pp. 201–264. Princeton.

SMITH, P. C. 1973 A similarity solution for slow viscous flow down an inclined plane. *J. Fluid Mech.* **58**, 275–288.

SPENCE, D. A. & SHARP, P. W. 1985 Self-similar solutions for elastohydrodynamic cavity flow. *Proc. R. Soc. Lond.* A **400**, 289–313.

SPENCE, D. A. & TURCOTTE, D. L. 1989 Buoyancy-driven magma fracture: a mechanism for ascent through the lithosphere and the emplacement of diamonds. *J. Geophys. Res.* (submitted).

SPERA, F. 1980 Aspects of magma transport. In *Physics of Magmatic Processes* (ed. R. B. Hargreaves), pp. 265–323. Princeton.

SWANSON, D. A., WRIGHT, T. L. & HELZ, R. T. 1975 Linear vent systems and estimated rates of magma production for the Yakima basalt on the Columbia Plateau. *Am. J. Sci.* **275**, 877–905.

WALKER, G. P. L. 1989 Gravitational (density) controls on volcanism, magma chambers and intrusions. *Austral. J. Earth Sci.* **36**, 149–165.

WEERTMAN, J. 1971 The theory of water-filled crevasses in glaciers applied to vertical magma transport beneath oceanic ridges. *J. Geophys. Res.* **76**, 1171–1183.